Copy 256

SECURITY INFORMATION

RM A53A09

NACA RM A53A09

6402

RESEARCH MEMORANDUM

BUFFETING OF A VERTICAL TAIL ON AN INCLINED BODY AT SUPERSONIC MACH NUMBERS

By Forrest E. Gowen

Ames Aeronautical Laboratory
Moffett Field, Calif.

[redacted]

NATIONAL ADVISORY COMMITTEE
FOR AERONAUTICS

WASHINGTON
March 24, 1953

RECEIPT SIGNATURE REQUIRED

[redacted]

319.98/13

[redacted]

NATIONAL ADVISORY COMMITTEE FOR AERONAUTICS

RESEARCH MEMORANDUM

BUFFETING OF A VERTICAL TAIL ON AN INCLINED BODY AT SUPERSONIC MACH NUMBERS

By Forrest E. Gowen

SUMMARY

Time histories of rolling and yawing moments on inclined bodies of revolution with vertical-tail surfaces were obtained at Mach numbers of 1.45, 1.98, and 2.90 and in the range of Reynolds numbers (based on body diameter) from 0.2 million to 1.3 million. Three ogival-nosed bodies (fineness ratio 5 tangent ogives) with over-all fineness ratios of 9.6, 12.0, and 14.4 and a conical-nosed body with a fineness ratio of 12.0 were tested. These tests were made in an angle-of-attack range from 0° to about 34° which included the angle-of-attack range where instability in the cross flow first occurred. The measurements of rolling and yawing moments were preceded by visual-flow studies of the cross-flow field at Mach numbers of 1.45 and 1.98 and supplemented at the same Mach numbers by time histories of the surface-pressure fluctuations on the body alone at a longitudinal station 10.6 diameters from the nose of the model. Typical records of both force and pressure measurements are included along with representative photographs of the cross-flow field obtained with schlieren apparatus and with the vapor-screen technique.

Although the side forces and yawing moments were small, it was found that large rolling moments which fluctuated in a random manner accompanied the changing vortex pattern in the cross-flow wake. These rolling-moment fluctuations were reduced in magnitude by increasing the Mach number or by changing the nose shape from a sharp conical nose (small apex-angle cone) to an ogival nose. Increasing the distance from the tip of the ogival nose to the tail position was found to result in an increase in the magnitude of the rolling-moment fluctuations and a reduction in the angle-of-attack range at which the fluctuations occurred. Large fluctuations of surface pressure were also found to accompany the aperiodic fluctuating cross-flow wake. These pressure variations were found to occur over most of the lee side of the body at a longitudinal station 10.6 diameters from the nose.

[redacted]

[redacted]

INTRODUCTION

It has long been recognized that the effects of viscosity have an important influence on the flow over inclined bodies of revolution. In fact, both the steady and unsteady forces and moments are influenced by these viscous effects. Recently, a practical semiempirical method for evaluating the steady-state forces and moments on a slender body of revolution has been developed by Allen in reference 1. However, no evaluation of the effects of viscosity on the unsteady forces has been made. In reference 2 an investigation of the nature of the flow in the wake of an inclined body was made with the aid of a visual-flow technique. In that investigation a pair of symmetrically disposed vortices was found on the lee side of an inclined body of revolution near the nose of the body. As the distance downstream from the nose was increased these vortices became asymmetric, and at stations far downstream from the nose the vortex pattern in the cross-flow plane had the appearance of a Kármán vortex street. At large angles of attack the entire cross-flow field in the wake became aperiodically unsteady. It is this unsteady nature of the flow in the wake of inclined bodies at large angles of attack that would be expected to result in erratic fluctuations in the rolling and yawing moments for a body-fin configuration having the fins immersed in the wake from the lifting forebody. One experimental investigation of this phenomenon (ref. 3) indicated large rolling oscillations for a fin-stabilized body of revolution at high angles of attack, and showed that the amplitude of these oscillations decreased with increasing Mach number.

The purposes of the present program were to investigate some of the effects of nose shape, longitudinal position of the tail, tail size, Reynolds number, and Mach number on the magnitudes and frequencies of the yawing and rolling moments associated with the asymmetry and instability of the vortex wake of a simple body-fin combination. The measurements of these yawing and rolling moments were to be supplemented by time histories of the surface-pressure fluctuations near the longitudinal position of the tail fin.

SYMBOLS

b tail span measured from body axis, in.

C_l rolling-moment coefficient, rolling moment/$q_o Sb$

ΔC_l maximum deviation of instantaneous rolling-moment coefficient from the average value of C_l

[redacted]

d maximum diameter of body, in.

l length of body, in.

l_n length of body nose, in.

M_o free-stream Mach number

P pressure coefficient, $\frac{p - p_o}{q_o}$

ΔP maximum variation of instantaneous pressure coefficient from average value of P

p local static pressure on body surface, lb/sq in.

p_o free-stream static pressure, lb/sq in.

q_o free-stream dynamic pressure, lb/sq in.

Re Reynolds number based on free-stream conditions and maximum body diameter

S plan-form area of vertical fin including the area projected to the body axis, sq in.

α angle of attack, deg

θ circumferential angle measured from the approach direction of the cross-flow velocity, deg

APPARATUS AND TESTS

Wind Tunnels

This investigation was conducted in the Ames 1- by 3-foot supersonic wind tunnels Nos. 1 and 2. The nozzles of these tunnels are similar and are equipped with flexible top and bottom plates. Tunnel No. 1 is a single-return, continuous-operation, variable-pressure wind tunnel with a maximum Mach number of 2.2. Tunnel No. 2 is an intermittent-operation, nonreturn, variable-pressure wind tunnel with a maximum Mach number of 3.8. The models were supported on conventional sting-type rear supports for the present tests.

[redacted]

Models

Sketches of the models used for the rolling- and yawing-moment measurements and those used for the surface-pressure measurements are shown in figure 1. The former were constructed so that with the ogival nose three cylindrical afterbodies of different lengths could be used in combination with either of two vertical tail fins, the larger shown by the solid lines in figure 1(a) and the smaller by the dotted lines. In addition, one conical-nosed model was constructed which could also be used in combination with the larger tail fin. These models were mounted on ball bearings attached to the sting support, and restrained in roll by a simple torsion member. Conventional strain gages were located on the torsional member and upon the sting to measure the rolling and yawing moments, respectively. The model used for studying surface-pressure fluctuations is shown in figure 1(b). Two capacitance-type pressure cells mounted in the cylindrical afterbody as shown were used to obtain time histories of the fluctuating surface pressures.

Instrumentation

Diagrams of the electrical instrumentation used for both the force and pressure measurements are presented in figure 2. The units of the carrier equipment (i.e., oscillator, bridge, amplifier, and detector shown schematically in fig. 2(a)) which were used in conjunction with the strain gages for obtaining the yawing and rolling moments are described in detail in reference 4. The output from each gage was used to modulate the 2000-cycle carrier wave which was then amplified and detected. With the exception of the output from the rolling-moment gage, the detected signals were recorded on a multichannel oscillograph. The output of the rolling-moment gage was divided into two parts and only the first part of the signal was recorded directly from the detector. The second part of the signal was passed through an integrating network which, in effect, filtered out that part of the signal due to the mechanical natural frequency of the system and indicated only the external disturbances (both random and periodic). The traces from both parts of the rolling-moment signal and from the outputs of the yawing-moment gages were recorded simultaneously. The frequency response of the system was limited primarily by the galvanometer elements in the oscillograph. The frequency response of these elements was flat within ±2 percent to 250 cycles per second and dropped to about 55 percent at 500 cps.

The electrical system used for measuring the surface-pressure fluctuations was similar to that described in reference 5 and is shown schematically in figure 2(b). Small changes in pressure caused the diaphragm of the pressure cell to deflect and alter the capacitance of the cell. This capacitance change caused the voltage drop across the resistance units in the circuit to vary with time. The voltage variation was then measured directly on the screen of an oscilloscope or recorded on film with an oscilloscope camera. The average pressure across the cell was balanced by applying a static pressure or suction to the diaphragm chamber of the cell. The high sensitivity and linearity of the cell could be maintained with this pressure-balancing method. The frequency response of the pressure-measuring system was limited primarily by the acoustic system in the model (i.e., the chamber and orifice above the pressure cell). This acoustic system was designed so that any fluctuations in pressure up to about 2500 cps could be measured without being affected by acoustic resonance. The response of the complete system was checked throughout a frequency range from a few cycles to over 2500 cps and found to be satisfactory.

Test Procedure

The investigation was conducted in three parts: first, a study of the cross-flow wake behind the body by means of the vapor-screen technique; second, a study of the time histories of rolling and yawing moments on the body and body-tail combination; and third, measurement of the surface-pressure fluctuations at one longitudinal station on the body. The test conditions for each of these phases of the investigation are given in table I.

Briefly, the vapor-screen method of flow visualization is as follows: A small amount of water is added to the tunnel to form a fine fog in the test section. High-intensity light from a narrow slit is passed through the test section forming a screen of visible fog particles. Disturbances in the flow are then indicated as variations in density of the light screen (referred to herein as "vapor screen"). Further details on this method are given in reference 2.

Prior to the measurement of the rolling and yawing moments on the model in the wind tunnel, several preliminary experiments and calibrations were necessary. These preliminary tests consisted of the following: initial calibrations of all gages, one wind-tunnel test of the body alone to determine temperature effects on the rolling- and yawing-moment gages (these effects were negligible), and bench tests of each model to determine its natural single-degree-of-freedom frequencies.

[redacted]

In general, for the wind-tunnel tests, time histories of the rolling and yawing moments were taken for 5- to 10-second intervals of time at as many angles of attack as were necessary to provide a representative sample of the maximum rolling and yawing moments obtainable within the available angle-of-attack range. Schlieren pictures were also taken at each angle of attack to provide information on both the model angle of attack and the wake vortices.

Since for the surface-pressure measurements the model attitude in both pitch and roll could be remotely controlled, preliminary surveys of the surface-pressure fluctuations around the body and throughout the angle-of-attack range were made to determine angles of attack at which data were to be taken. This survey was necessary to insure that records representative of the maximum fluctuating surface pressures were obtained. The magnitudes of the pressure fluctuations were measured directly from the oscilloscope screen or were recorded photographically in those instances where the pressure fluctuations were large. The average static pressures on the pressure cell were measured by a manometer.

REDUCTION OF DATA

Rolling- and Yawing-Moment Measurements

Measurements of the rolling and yawing moments were obtained from records similar to those presented in figure 3. Typical sections of a series of records of the time histories of these measurements for a conical-nosed body at various angles of attack are shown in figure 3(a). Figure 3(b) shows a longer section of one particular record for the ogival-nosed body. This record is essentially the same as those shown in figure 3(a) except that a filtered rolling-moment trace was added to the record. This trace indicates the output from the electronic filter network which transmitted only the fluctuating component of the rolling moments and filtered out those rolling moments that occurred at the natural rolling frequency of the model. The magnitudes of the rolling moment were evaluated using a static calibration of the rolling-moment gage. No correction was made for the small change in gage frequency response between 0 and 250 cps or the reduction in response at higher frequencies. The measurements of the average rolling moments were obtained from the mean value of the unfiltered rolling-moment trace over the time intervals of the records and, except in the angle-of-attack range where large rolling fluctuations occurred, the uncertainty in the magnitudes of the resulting rolling-moment coefficients is estimated to be of the order of ± 0.002. The value of the maximum oscillating rolling moment at each angle of attack was obtained from the filtered rolling-moment trace and is given throughout this report as the maximum single amplitude deviation from the mean. An uncertainty of the order of

[redacted]

±25 percent was involved in the measurements of this oscillating component of rolling moment as a result of the variation of the electronic-filter-network calibration constant with both frequency and magnitude of the forcing function. In spite of this large possible error in the individual measurements of the oscillating rolling moment, the important results (i.e., order-of-magnitude changes in the rolling-moment fluctuations) were not obscured, because the large changes in rolling moment that were associated with variations in vortex asymmetry and instability were indicated on the record in such a manner as to be unmistakably evident. (See, for example, the variations in rolling moment shown by the records in fig. 3.)

Since both the frequency and the magnitudes of the rolling moments are important, all of the predominate frequencies indicated on the records were noted for possible correlation. It was found that during most of the tests the models were vibrating at frequencies about 40 or 50 percent above their natural single-degree-of-freedom frequencies. These frequencies were also found in the wind-tunnel tests of the models without tail surfaces installed and in a few of the bench calibrations. Therefore, it was concluded that this frequency was associated with model vibration in more than one degree of freedom rather than with any periodic external force.

Surface-Pressure Measurements

Time histories of the fluctuating component of surface pressure were obtained around the test bodies for both steady and unsteady flow in the wake. Typical sections of a few of these records are shown in figure 4. The maximum fluctuations in the surface pressure have been reduced to single-amplitude or deviation-from-the-mean coefficients. The errors in the individual values of the average and the fluctuating components of the pressure coefficients have been calculated from the uncertainties in the measurements and calibration constants and may be as much as ±10 percent throughout the range of test conditions.

RESULTS AND DISCUSSION

This investigation has been conducted in three phases, namely, the visual-flow study, measurement of the rolling and yawing moments, and measurement of the surface pressure fluctuations. The following discussion will consider each of these phases and compare their results wherever possible.

Visual-Flow Studies

It has been generally observed that a stable symmetric pair of vortices is associated with a lifting body of revolution at low angles of attack. (See, for example, refs. 2 and 3.) As the angle of attack of the body increases, this vortex configuration becomes asymmetric and then unsteady. In figure 5 typical symmetric and asymmetric vortex patterns are shown for a body with an ogival nose and a body with a slender conical nose. These vapor-screen pictures, which were taken with the light screen at the approximate location of the trailing edge of the tail on the models,[1] show that the vortex configuration associated with the ogival-nosed body remained symmetric to a much greater angle of attack than did the configuration for the slender conical nose. Although this difference was found for these particular models, the results are not generally applicable to all cones and ogives because it has been found that increasing the apex angle of the conical nose results in a change in vortex pattern toward that of an ogive.[2] However, even though it appears that the apex angle is an important parameter, additional tests are needed to verify this effect.

At large angles of attack, the asymmetry in the cross-flow vortex configuration shown for the two models in figure 5 might be expected to result in yawing moments on the bodies and rolling moments on fins submerged in these cross-flow wakes. Similarly, unsteadiness in the vortex pattern would give rise to both unsteady yawing and rolling moments. Each of the models tested in the high angle-of-attack range (i.e., 28° or 30° and greater) were observed to have asymmetric and aperiodically unsteady vortex patterns in the wake similar to those shown in figure 6. These pictures are sequences taken from a movie and show the change in vortex configuration with time at two angles of attack for the body with the ogival nose. The movies were taken at 10 frames per second and illustrate the rapidity with which the vortex configuration, and hence the induced rolling moment on any fin placed in the cross-flow wake, may change in the high angle-of-attack range. At an angle of attack of 28° this change in vortex pattern occurs between the various frames, but one frame of the sequence for an angle of attack of 36° (third from bottom) shows that within the exposure time for that single frame the vortex configuration changed.

The preceding discussion has been concerned with variations in the vortex configuration at one station near the base of the body. However,

[1] The tail fin was removed for the vapor-screen studies to eliminate the complication of the picture by the shadow of the vertical-tail surface.

[2] Results of several tests have shown that for a 19° apex-angle conical nose (approximately a fineness ratio 3 nose) the wake pattern was very similar to that for a fineness ratio 5 ogival nose.

development of the cross flow between the nose of a body and the base may also be important if forward control surfaces, ducts, external equipment, or bodies of various lengths are to be considered. This development of the cross flow with distance along the body can be observed by moving the light screen along the body (fig. 7) or by tracing the vortex cores (broad dark lines in the lee of the body) in schlieren photographs such as those of figure 8. It is interesting to note that the variation of the vortex pattern with distance from the nose shown in figure 7(a) is somewhat similar to the variation with angle of attack shown in figure 5(a) for the same model. The schlieren picture in figure 8(a) shows a single symmetric vortex pair as one continuous line which diverges slightly from the body with distance from the nose. A staggered arrangement of vortices is indicated as a series of branching lines such as those shown in figures 8(b) and 9(a) for a conical-nosed body. From a study of these and other schlieren photographs, it has been found that the distance from the nose at which the change from a symmetric vortex pair to an asymmetric configuration of two or more vortices occurs decreases as the angle of attack increases.

Several vapor-screen tests have indicated that minute irregularities in the sharp nose of the conical-nosed model may affect the symmetry of the vortex pattern. An example of this effect is shown by the schlieren photographs in figure 9 which were taken at identical free-stream conditions. The only difference in the test conditions for the two photographs was that the model had been rolled approximately 10° about its longitudinal axis. The two pictures indicate entirely different vortex configurations in the wake. After these pictures were taken a careful examination of the model revealed a minute rotational asymmetry within about the first 0.020 of an inch of the tip of the model.[S] Hence, in the cross-flow plane near the tip, the model presented an asymmetric profile to the oncoming cross flow which resulted in the asymmetry in the wake shown in figure 9(a). Thus it appears that any small irregularities, or lack of rotational symmetry, in the vicinity of the tip of a very slender pointed body where the boundary layer is thin can affect the vortex configuration in the cross-flow wake.

The effects of Reynolds number and Mach number on the vortex configuration were studied for the bodies of revolution used in this investigation. For a given free-stream Mach number and distance from the nose it was found that, in general, an increase in Reynolds number was accompanied by a reduction in the angles of attack at which the asymmetry and the instability of the vortex pattern occurred. This

[S]The irregularity in rotational symmetry encountered in these tests extended from the tip of the cone about 0.02 or 0.03 inch toward the base. In this region, a section of the cone perpendicular to its axis was circular except for one slightly flattened side which was smoothly faired into the circular arc. This flattening caused the tip of the model to be about 0.0004 inch from the original cone axis.

[redacted]

effect was most pronounced in the lower Reynolds number range (approximately 0.2 million) and decreased with increasing Reynolds number. For Reynolds numbers of 0.5 or 0.6 million there was little effect. For a given Reynolds number an increase in free-stream Mach number from 1.45 to 1.98 was accompanied by a 3° to 5° increase in the angle of attack at which the vortex pattern first became asymmetric. A similar increase was found for the angle of attack at which instability in the cross-flow wake occurred.

Since correlations were to be made between the results of the visual-flow studies and the measurements of the rolling and yawing moments, it was necessary to determine the effects of water particles in the free stream on the vortex pattern. It was noted during the visual-flow study that a considerable increase in the visible water-particle density above that usually used for the vapor-screen tests caused a decrease in the angle of attack at which instability in the cross flow occurred. If a similar effect were to occur when the water content of the free stream was increased from the minimum used for the rolling- and yawing-moment tests[4] to that used for the visual-flow studies, it is apparent that no correlation would have been possible. However, comparison of the rolling and yawing moments obtained from two force tests, one made with a specific humidity similar to that used during the vapor-screen tests and the other with a minimum specific humidity, revealed no significant difference. Therefore, it was concluded that for the water-particle density used in the visual-flow studies the vortex configuration was essentially unaltered by the presence of the water particles.

Rolling- and Yawing-Moment Measurements

The results obtained from the present investigation should be considered more qualitative than quantitative because of the limitations necessarily imposed upon wind-tunnel tests of this type. Three of the factors which may limit the applicability of these results to full-scale aircraft are as follows: First, vibrations transmitted to the model from its mounting system may influence the shedding of the vortices; second, model structural rigidity or its stiffness relative to a full-scale vehicle may be important; third, the possibility of coupling between the motion of the full-scale vehicle and the shedding of its vortices could give rise to results different from those obtained for the wind-tunnel model which is restrained by its mounting system. Even though the absolute magnitudes of the measured moments may have little application to full-scale design problems, the trends with a number of

[4]The absolute humidity during the rolling- and yawing-moment tests was of the order of 0.0002 pound of water per pound of dry air.

[redacted]

variables such as Mach number, Reynolds number, and angle of attack are believed significant. Hence, the following results of the rolling-moment measurements are presented to indicate the nature of these trends. The yawing-moment measurements will not be duscussed in detail, since the data on the magnitude and frequency of these lateral oscillations did not indicate clearly defined trends with the major variables. The magnitudes of the yawing moments and side forces obtained from the two yawing-moment traces were small, and hence the sensitivity of the gages was not sufficient to obtain accurate measurements of these characteristics. In fact, the side forces (including both aerodynamic and inertia forces) were less than the equivalent lift that would be developed by a similar body at an angle of attack of only 3° or 4°. The lateral oscillations of the model were found to occur at the natural single-degree-of-freedom frequency of the model in the yaw plane for all of the tests.

Angle-of-attack effects.- In general, the tests of all of the models used in the present investigation exhibited a similar sequence of events with increasing angle of attack. Changes in the vortex configuration (indicated in the visual-flow studies) were accompanied by changes in the rolling-moment characteristics of models with vertical-tail fins immersed in the cross-flow wake. As soon as any asymmetry in the cross-flow field developed, rolling moments were induced on the models. As the cross-flow asymmetry became more pronounced and the wake became unsteady, the rolling moments increased and finally became unsteady. In some instances, above the angle of attack at which unsteadiness in the cross flow first occurred, increases in angle of attack were accompanied by variations in rolling moments from fairly steady to wildly oscillating to fairly steady again (e.g., fig. 3(a)). It was noted that the vortex patterns associated with these variations were most unsteady during the appearance of an additional vortex in the cross-flow field. For example, as the vortex pattern changed from one containing three vortices to one containing four vortices, the flow was extremely unsteady compared to the flow where a specified number of vortices existed in the field. Even though there were similarities in the sequence of events with increasing angle of attack for the various tests, it was apparent that in some instances there were large differences in both the magnitudes of the rolling moments (the average and fluctuating components of the rolling moment) and the angle-of-attack ranges at which the unsteady rolling moments occurred (e.g., different Mach numbers in fig. 10).

Mach number effects.- In reference 3, it was reported that the amplitudes of the rolling-moment fluctuations were reduced as the Mach number was increased in the range of Mach numbers from 0.9 to 1.7. A similar effect of Mach number was found in the results of the present investigation (fig. 10) for both the average and the maximum-fluctuating components of the rolling moment for Mach numbers of 1.45, 1.98, and 2.90. This effect was not necessarily a reduction at each angle of attack,

[redacted]

but a reduction in the maximum rolling-moment coefficients obtained within the available angle-of-attack range. The reduction in magnitude of the maximum rolling-moment-coefficient fluctuations between Mach numbers of 1.98 and 2.90 may be even greater than that shown because of the difference in Reynolds number. (The effects of Reynolds number will be discussed later.) As was noted in the visual-flow studies, increasing the Mach number from 1.45 to 1.98 increased the angle of attack at which unsteadiness in the cross flow occurred. This angle of attack is characterized by a sudden rise in the rolling-moment fluctuations with increasing angle of attack such as that shown in figure 10 at about 26-1/2° for a Mach number of 1.45. Although the angle at which unsteadiness first occurred increased in the Mach number range from 1.45 to 1.98 (an effect also indicated by the data of ref. 3), comparison with the data at a Mach number of 2.90 indicates a reversal of this trend. However, because of the difference in Reynolds number between the tests at Mach numbers of 1.98 and 2.90 and in view of the possible Reynolds number effect on the angle of attack at which unsteadiness occurs, no conclusive trend with Mach number can be established above a Mach number of 1.98. An additional factor which may influence the results is the probable difference in free-stream turbulence[5] between the tests in tunnel No. 1 and the test at a Mach number of 2.90 in tunnel No. 2. Since the phenomenon being studied involves an unsteady-flow problem, it might be expected that the turbulence level of the free stream could have a large effect on the results.

Reynolds number effects.- Results of a series of tests conducted with the conical-nosed model for a range of Reynolds numbers at a free-stream Mach number of 1.98 are shown in figure 11. Data for the lower Reynolds numbers were obtained in tunnel No. 1 (figs. 11(a) and 11(b)), and for the higher Reynolds numbers in tunnel No. 2 (figs. 11(c) and 11(d)). It is apparent from the results of the tests in tunnel No. 1 that as the Reynolds number was increased from 0.2 million to 0.5 million, the angle of attack at which large average rolling moments occurred was decreased and the magnitude of the fluctuating component of the rolling moment was increased. However, further increases in Reynolds number from 0.5 million to 1.3 million (tunnel No. 2 data, figs. 11(c) and 11(d)) do not clearly indicate the same trends. Even though the major fluctuations in rolling moment for the higher Reynolds number tests occurred at about the same angle of attack, the data indicate a generally

[5]A difference in turbulence level between tunnels No. 1 and No. 2 has been indicated in the results of recovery-temperature measurements made on a thin-walled 10° cone in both tunnels (figs. 2 and 5 of ref. 6). These results show that the Reynolds number for transition from laminar to turbulent boundary-layer flow is considerably lower in tunnel No. 2. Although no measurements of absolute turbulence level (e.g., hot-wire measurements) have been made in either tunnel, this difference in the Reynolds number for boundary-layer transition is believed to have been caused by a difference in turbulence level.

higher level of rolling-moment fluctuations over the entire angle-of-attack range. This higher level of fluctuations might be associated with some differences in the free-stream conditions (such as turbulence level) for the two tunnels. Any such changes in flow apparently had little influence on the average rolling-moment coefficients since, below the angle at which large unsteadiness occurs, rolling-moment coefficients obtained in tunnel No. 2 (fig. 11(c)) were quite similar to those of the higher Reynolds number data in tunnel No. 1 (fig. 11(a)). The only difference between the average rolling-moment data for a Reynolds number of 0.5 million (fig. 11(a)) and the data for the higher Reynolds numbers (fig. (fig. 11(c)) is that the direction of the rolling moment is different for angles of attack below that for which major rolling-moment fluctuations occurred. Since the sign of the average rolling-moment coefficient is determined by the asymmetry of the vortex pattern (see fig. 5) and since the initial asymmetry may occur with either vortex being the closer to the body, it is possible to have average rolling-moment coefficients with either sign on a particular test. In fact, repeat tests with the same model at different times have indicated rolling moments with similar magnitudes but with reversed sign. The mechanism which controls the longitudinal position of the separation point on either side of a symmetric body (and hence the symmetry or asymmetry of the vortex pattern) is not understood. However, it is very likely that a number of factors, such as a minute irregularity in the tip shape or nonuniformities in flow conditions, could cause the asymmetry to occur in a given manner for a given set of test conditions. In the angle-of-attack range where the unsteadiness occurred, as would be expected from the vapor-screen studies, there were large variations in the average rolling moments and sudden changes with increasing angles of attack.

Nose-shape effects.- The rolling moments were measured on one model consisting of a cylindrical afterbody that could be used in combination with either a conical or ogival nose. The results are shown in figure 12 for a Mach number of 1.98. Comparison of average rolling-moment coefficients for the two nose shapes shows that even though the values of the maximum average rolling-moment coefficients due to flow asymmetry are of the same order of magnitude, the variation with angle of attack for the ogival-nosed model is not nearly as erratic as that for the conical-nosed model. The fluctuating component of the rolling-moment coefficients for both models were small at angles of attack below about 14°. However, the maximum values of the fluctuating component of rolling moment obtained within the available angle-of-attack range were not small, and for the conical-nosed body were about four times those obtained for the body with the ogival nose. These results are in general agreement with the indications from vapor-screen tests where it was observed that for the model with the ogival nose, the flow in the cross-flow wake was more steady and the vortex configuration symmetric to higher angles of attack than for the model with the sharp conical nose (i.e., a cone of small apex angle). Thus, the change in nose shape from a sharp conical nose to an

ogival nose would be expected to alleviate some of the roll-control difficulties which might be experienced at moderate angles of attack by a missile with vertical stabilizing surfaces in the cross-flow wake.

Effect of vertical-tail location.- One series of tests was made at a Mach number of 2.90 and a Reynolds number of 0.7 million to determine the effect of the longitudinal position of the tail on the fluctuating rolling moments for the model with an ogival nose. The results of these tests are presented in figure 13[6] for three longitudinal positions of the tail. As the distance from the nose to the tail was increased, two effects were observed. There was an increase in the magnitude of the maximum fluctuating component of rolling moment and a reduction in the angle of attack at which the major fluctuations occurred. This latter effect is in qualitative agreement with the results of the visual-flow study on the ogival-nosed body (figs. 5 and 7).

Throughout this report all the curves for the fluctuating component of rolling-moment coefficient have been drawn through each of the test points to indicate the large changes in rolling fluctuations that occur with small changes in angle of attack for a particular test. This effect is clearly illustrated by the data of figure 13(b). However, it might be expected that if a number of repeat tests of the model of figure 13(b) were made, each test could indicate similar sudden violent rolling fluctuations with small changes in angle in the same angle-of-attack range, but not necessarily at exactly the same angle of attack, or of exactly the same magnitude as shown in the figure.

For all positions of the vertical tail considered in figure 13, the values of the average rolling-moment coefficient were, in general, less than those shown in figures 10 to 12.

Effect of tail size.- Tests of the ogival-nosed body were conducted at a Mach number of 2.90 and a Reynolds number of 0.7 million with two different sized tail fins. The results of these tests indicated that the reduction in tail size was accompanied by a reduction in magnitude of the fluctuating component of rolling-moment coefficient. In fact, no significant fluctuations were recorded for any of the tests with the small fin at any angle of attack. In the angle-of-attack ranges where rolling-moment fluctuations might have occurred, schlieren pictures of the wake indicated that the vortex cores were above the tip of the tail fin. Thus, the tail was probably out of the region where the major influence of the vortex fluctuations occurred. Also, during these tests with the small tail there were appreciable zero shifts on the output from the rolling-moment circuit which resulted in considerable uncertainty in the values of the average rolling-moment coefficients. Therefore, no conclusions as to the effects of tail size on the average rolling-moment coefficients could be made, and the data are not presented.

[6]Note that in this figure the ordinate scale is different from that of the previous figures.

[redacted]

Pressure Measurements

Since frequencies in the unsteady cross flow greater than about 600 or 700 cps could not be detected by either the vapor-screen method or the equipment used to record the rolling and yawing moments, the measurement of the instantaneous surface pressures was undertaken to extend the frequency range up to about 2000 or 3000 cps. These measurements were made at one longitudinal station on the fineness ratio 12 body near the tail-surface position. (The tail surface was removed for these tests.) These tests provided information on both the magnitude and time history of the pressure fluctuations which occurred as well as the circumferential extent of the region of the body subjected to these pressure fluctuations.

Three short sections of the oscillograph records have been reproduced in figure 4 to illustrate the nature of the surface-pressure fluctuations. A few of the records (e.g., figs 4(a) and 4(b)) indicated that changes in pressure coefficient of the order of 0.2 occurred within a time interval of about 0.002 second, and in some instances pressure changes appeared to occur in a much shorter time interval. All pressure fluctuations appeared to be completely random and no predominant or characteristic frequency could be found on any of the pressure records. Circumferential distributions of average pressure coefficient with the maximum fluctuations in pressure coefficient superimposed are shown in figure 14 for two angles of attack at a Mach number of 1.45. These results for an angle of attack of 15° are typical for all models at low angles of attack and show merely the order of magnitude of the noise level (both acoustic and electronic) relative to the average surface-pressure coefficient. The data shown for an angle of attack of 32° are typical of the results obtained for models with a fluctuating cross-flow wake. The pressure variations over the windward side of the body were similar to those obtained at lower angles, but over the lee side of the body the total fluctuations of pressure coefficient were as large as the average pressure coefficient in some parts of this region. These data also indicate that at this longitudinal station the region of influence of surface-pressure fluctuations extends over the entire lee side and a small part of the windward side of the model. Results for other test conditions (fig. 15) also showed similar regions of influence wherever large variations in pressure were observed.

The circumferential distributions of the fluctuating component of surface-pressure coefficient obtained at a station 10.6 diameters from the tips of the conical-nosed body and the ogival-nosed body are presented in figure 15 for several angles of attack and a Mach number of 1.45. Although the data at all angles of attack are not shown, except for the angle-of-attack range of about 22° to 28°, the magnitudes of the pressure fluctuations for both nose shapes were quite similar and increased in magnitude with increasing angle of attack above about 15° to 18°. In

the range of angles of attack from 22° to about 27°, the data for the conical-nosed body were influenced by a slight rotational asymmetry near the tip of the model. (See footnote 3.) This rotational asymmetry, although minute in size, affected the vortex pattern in the cross-flow wake. (See fig. 9.) At large angles of attack, where cross-flow instability occurred, this tip asymmetry caused a variation in the magnitudes of the maximum pressure fluctuations as the model was rotated to various positions in roll. The two dotted curves shown for an angle of attack of 27° indicate the two different levels of maximum pressure fluctuations which were found.

These results from the measurements of the pressure fluctuations on a body with two interchangeable noses are in qualitative agreement with the results of the visual-flow study. Also, for cases where comparisons can be made, the results are in qualitative agreement with the rolling-moment data for this Mach number (e.g., fig. 10).

Since the rolling-moment fluctuations were greatly reduced when the Mach number was increased from 1.45 to 1.98, a similar trend should be shown by the pressure measurements. The typical circumferential distributions of the pressure fluctuations at these two Mach numbers shown in figure 16 for the conical-nosed body indicate that not only were the pressure fluctuations reduced on the lee side of the body, but on the windward side also.

CONCLUDING REMARKS

It is apparent that even though the results obtained from the present investigation are more of a qualitative than quantitative nature certain definite trends have been established. For a body of revolution at a large angle of attack there was an unsteady vortex pattern in the cross-flow wake. When a vertical-tail fin installed on the body was exposed to this unsteady wake, no appreciable side forces or yawing moments were found; however, large rolling moments which fluctuated in a random manner did occur. These rolling-moment fluctuations were reduced in magnitude by increasing the Mach number, changing the nose shape from a sharp conical (small apex-angle cone) to an ogival nose, reducing the tail size, and reducing the distance from the nose to the tail position. In the range of angles of attack where cross-flow unsteadiness occurred, small changes in the angle of attack caused large changes in the average rolling moment and in the rolling-moment fluctuations. The aperiodic nature of this unsteadiness in the cross flow (found in the time histories of the rolling moments) was substantiated by measurements of the time histories of the surface-pressure fluctuations at a station 10.6 diameters from the nose of the body. At this longitudinal station, the surface-pressure fluctuations were found to extend over the entire lee side of the body at angles of attack where cross-flow unsteadiness occurred.

[redacted]

The results show that small deviations from axial symmetry near the tip of a body, where the boundary layer is thin, can cause large changes in the downstream vortex pattern.

Ames Aeronautical Laboratory
National Advisory Committee for Aeronautics
Moffett Field, Calif.

REFERENCES

1. Allen, H. Julian: Estimation of the Forces and Moments Acting on Inclined Bodies of Revolution of High Fineness Ratio. NACA RM A9I26, 1949.

2. Allen, H. Julian, and Perkins, Edward W.: Characteristics of Flow Over Inclined Bodies of Revolution. NACA RM A50L07, 1951.

3. Mead, Merrill H.: Observations of Unsteady Flow Phenomena for an Inclined Body Fitted with Stabilizing Fins. NACA RM A51K05, 1952.

4. Erickson, Albert L., and Robinson, Robert C.: Some Preliminary Results in the Determination of Aerodynamic Derivatives of Control Surfaces in the Transonic Speed Range by Means of a Flush-Type Electrical Pressure Cell. NACA RM A8H03, 1948.

5. Wrathall, Taft: Miniature Pressure Cells. Paper presented at the Instrument Soc. of Amer. Conference and Exhibit, Cleveland, Ohio, Sept. 8, 1952.

6. Stine, Howard A., and Scherrer, Richard: Experimental Investigation of the Turbulent-Boundary-Layer Temperature-Recovery Factor on Bodies of Revolution at Mach Numbers of 2.0 to 3.8. NACA TN 2664, 1952.

[redacted]

TABLE I.- TEST CONDITIONS

Model nose	M_o	l_n/d	l/d	b/d	Re (million)	α (deg)
Visual-flow studies						
Ogive	1.98	5	12.0	-	0.5	9 to 33
Cone	↓	3	7.0	-	0.2 to 1.0	↓
↓	1.45	5	12.0	-	0.5	
		5	12.0	-	0.5	
Rolling- and yawing-moment measurements						
Ogive	2.90	5	9.6	-	0.7	9 to 31
↓	↓	↓	↓	1.5	↓	↓
				2.5		
			12.0	-		
			↓	1.5		
				2.5		
			14.4	1.5		9 to 30
			14.4	2.5	↓	9 to 30
	1.98		12.0	↓	0.8	9 to 33
Cone	2.90		↓		0.7	9 to 31
	1.98				0.2 to 1.3	17 to 33
↓	1.45	↓	↓	↓	0.5	9 to 32
Pressure measurements						
Ogive	1.98	5	12.0	-	0.5	15 to 32.5
Cone	1.98	↓	↓	-	↓	↓
Cone	1.45			-		

NACA

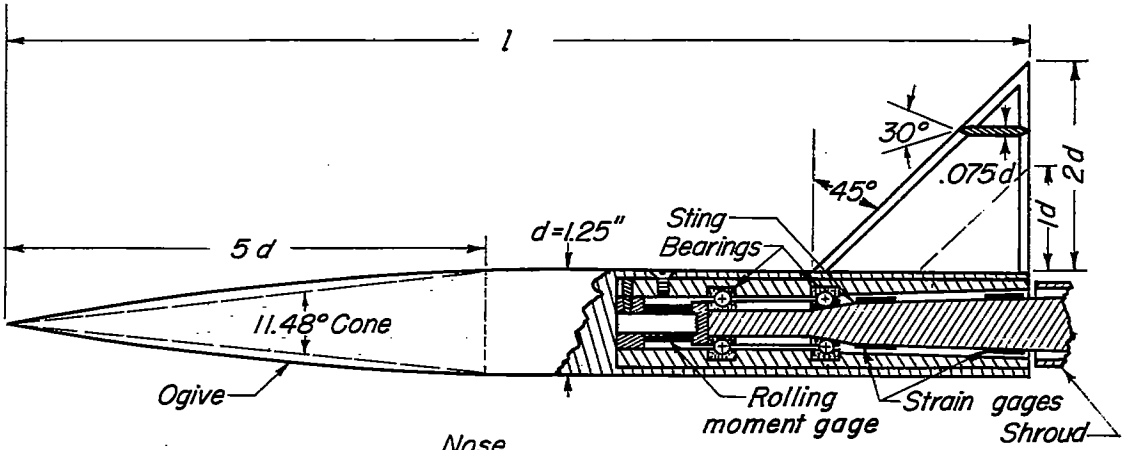

Nose shape	l/d
Ogive	9.6
Ogive	12.0
Ogive	14.4
Cone	12.0

(a) Models for rolling- and yawing-moment measurements.

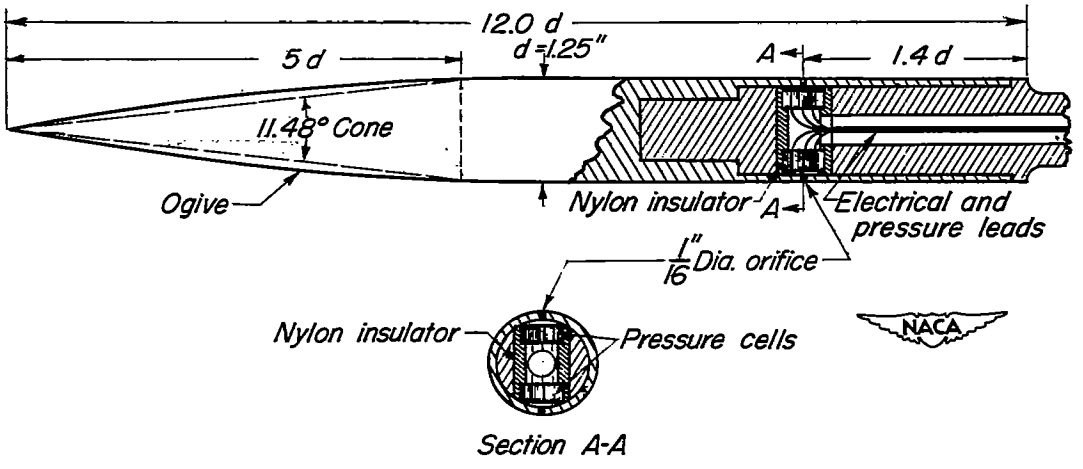

(b) Models for surface-pressure measurements

Figure 1.—Sketches of models.

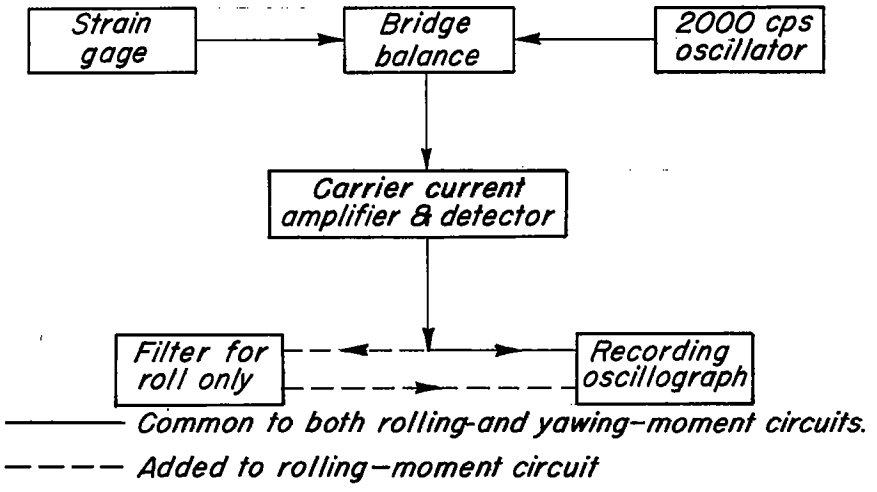

(a) Block diagram of moment recording system.

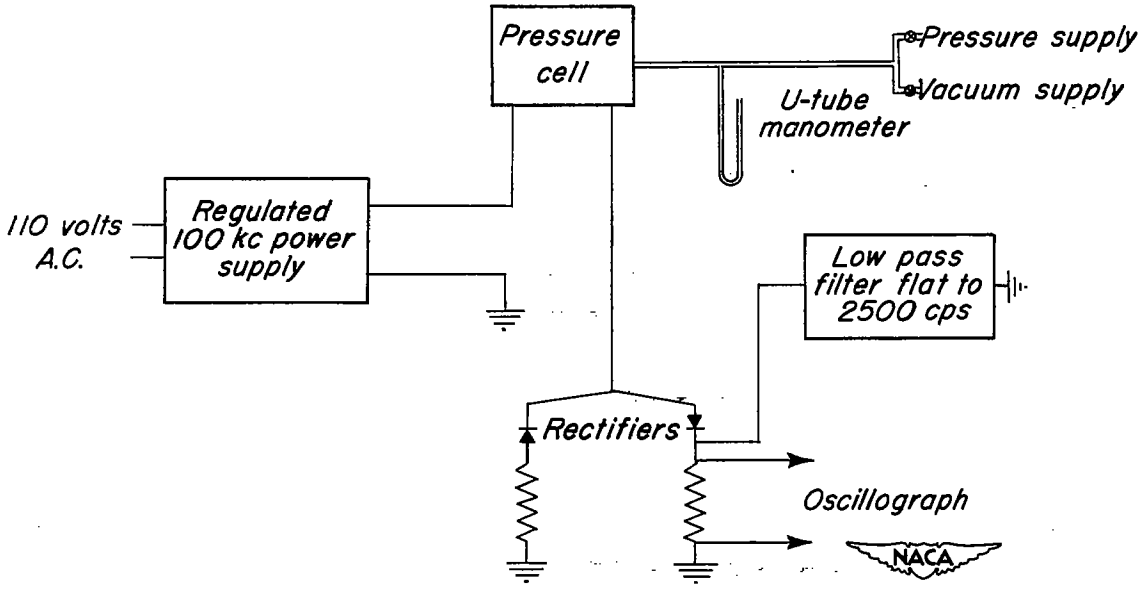

(b) Schematic diagram of pressure measuring system.

Figure 2.- Electrical instrumentation for tests.

[redacted]

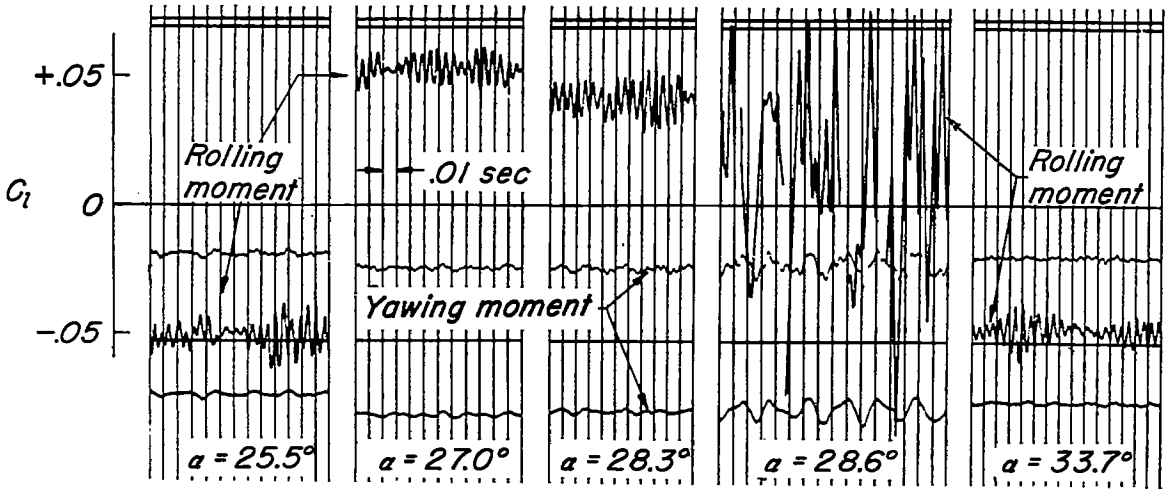

(a) Conical-nosed model, $M_o = 1.98$, $Re = 0.5 \times 10^6$.

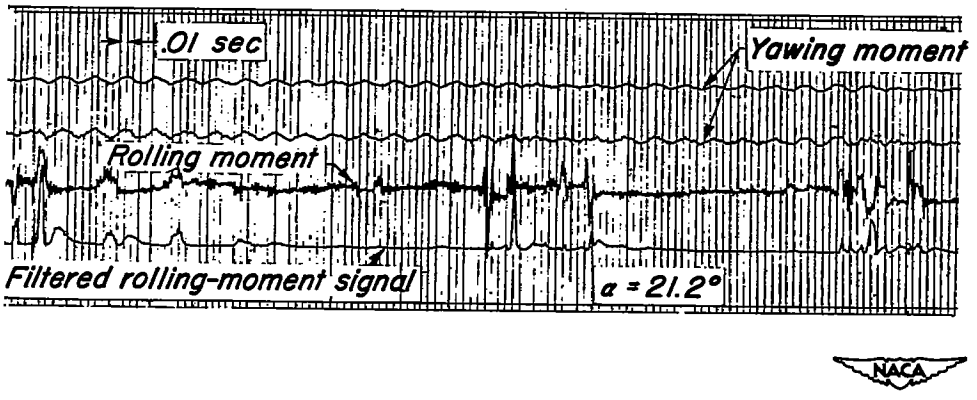

(b) Ogival-nosed model, $M_o = 2.90$, $Re = 0.8 \times 10^6$.

Figure 3.- Typical oscillograph records of the variation of rolling and yawing moments with time for several test conditions.

[redacted]

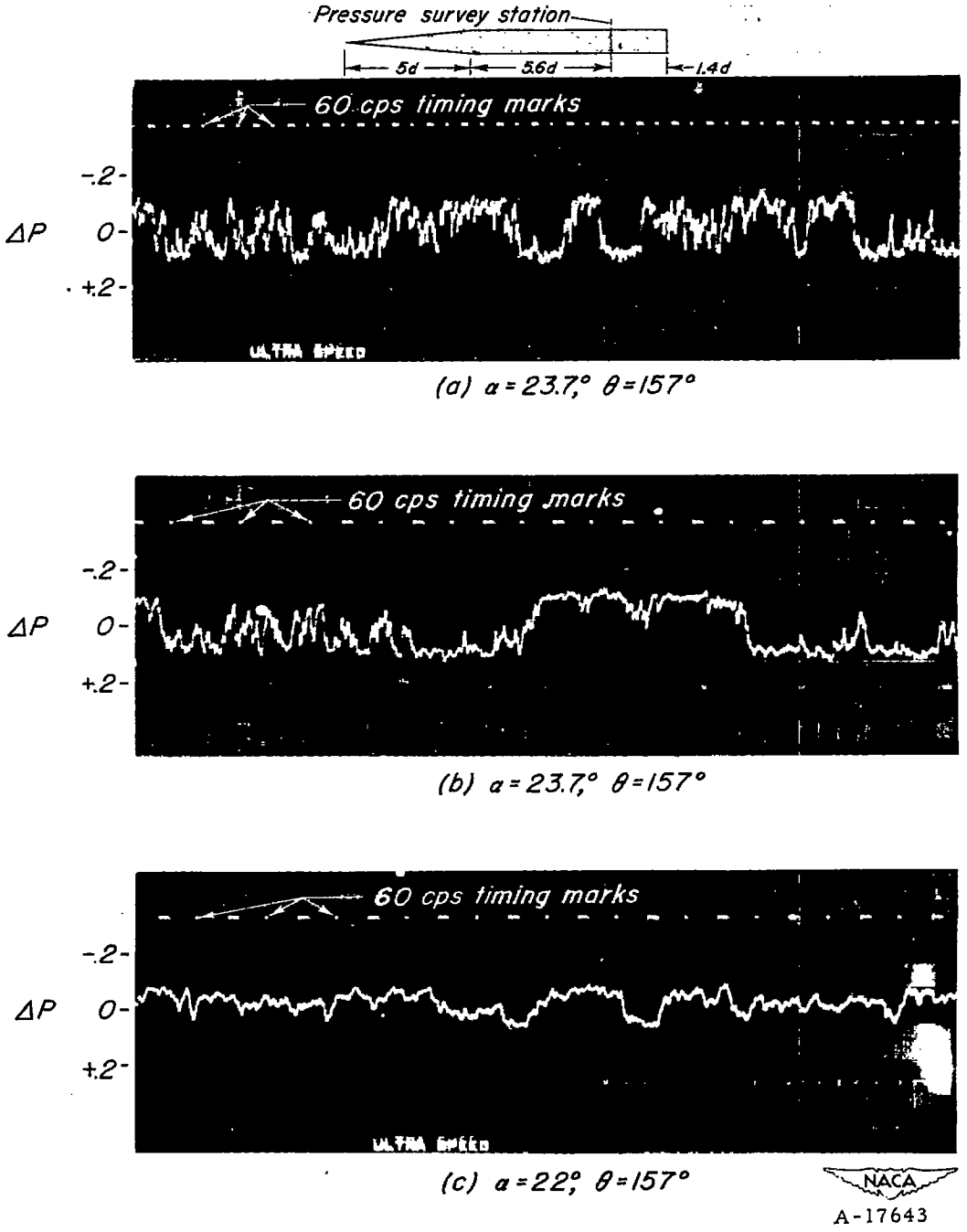

Figure 4.–Typical records showing the variation of pressure coefficient with time at one station on the conical-nosed body. $M_\infty = 1.45$, $Re = 0.5 \times 10^6$

[redacted]

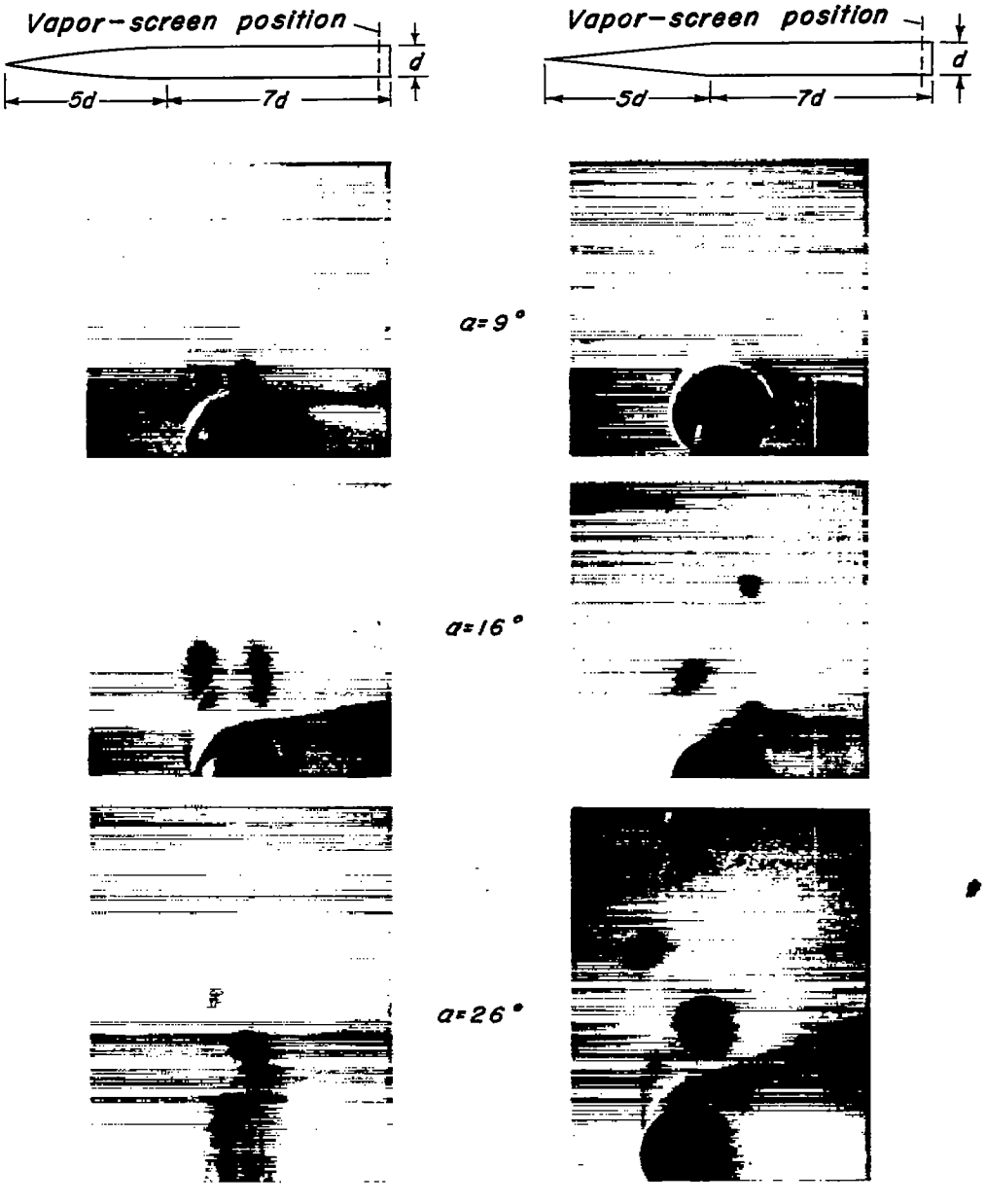

(a) Ogival-nosed body (b) Conical-nosed body

Figure 5.- Vapor-screen pictures showing the effect of nose shape on the variation of the vortex configuration with angle of attack. $M_o = 1.98$, $Re = 0.5 \times 10^6$

NACA
A-17638

[redacted]

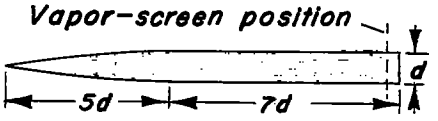

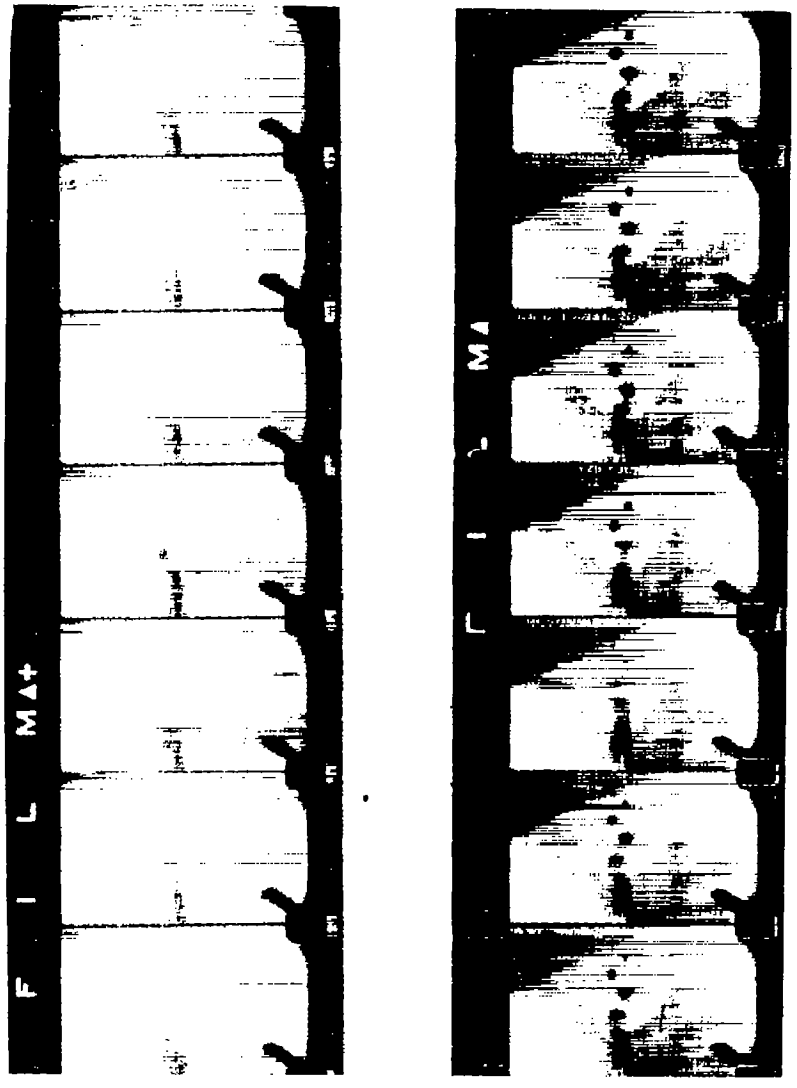

(a) $\alpha = 28°$ (b) $\alpha = 36°$

NACA
A-17639

Figure 6. - Vapor-screen movie sequences showing the fluctuation of the vortices in the cross-flow wake of an inclined body with an ogival nose. $M_\infty = 1.98$, $Re = 0.5 \times 10^6$

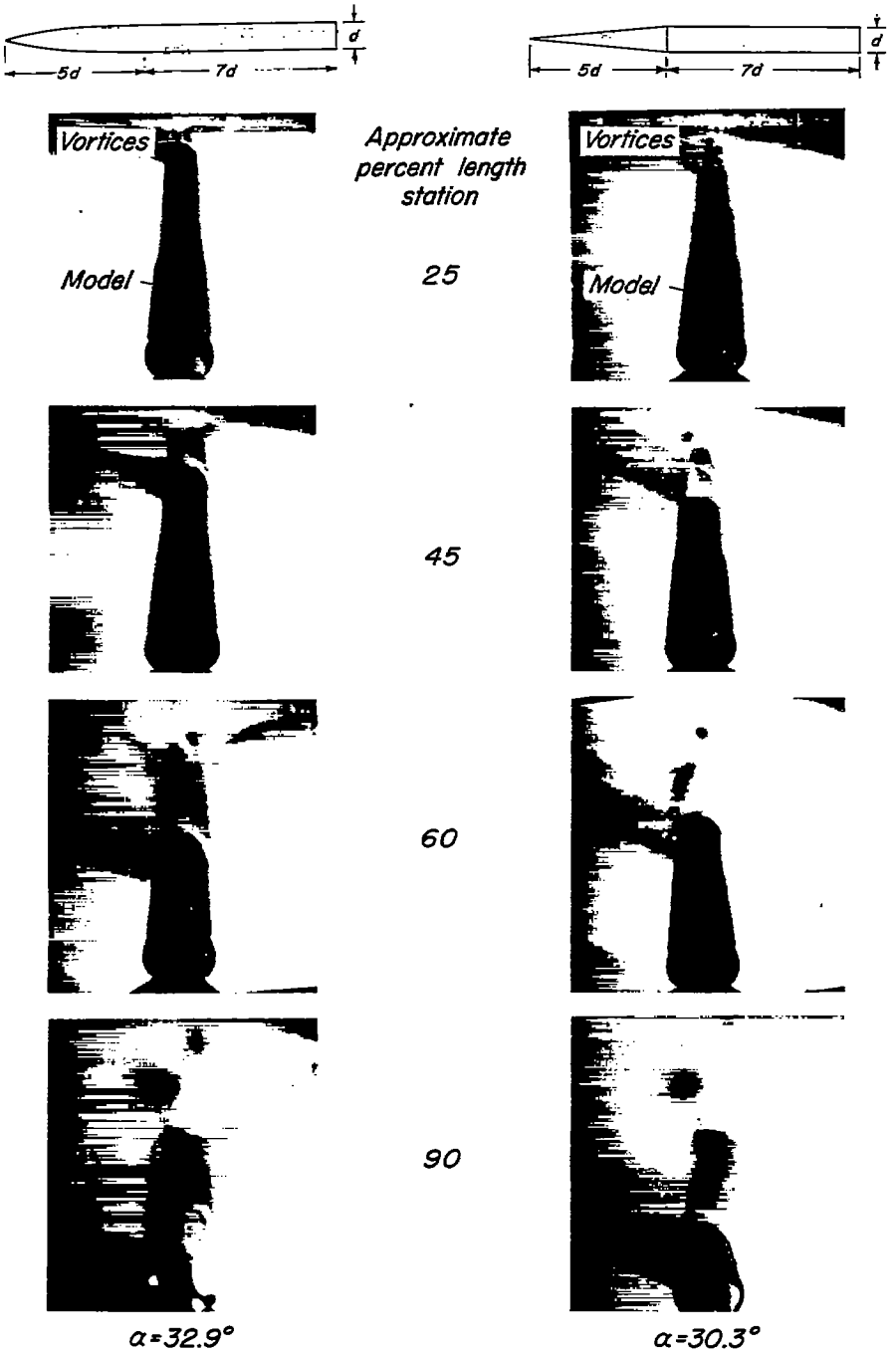

α=32.9°
(a) Ogival-nosed body

α=30.3°
(b) Conical-nosed body

Figure 7.—Vapor-screen pictures of the cross-flow vortices at various length stations on two bodies of revolution. $M_\infty = 1.98$, $Re = 0.5 \times 10^6$

NACA
A-17640

[redacted]

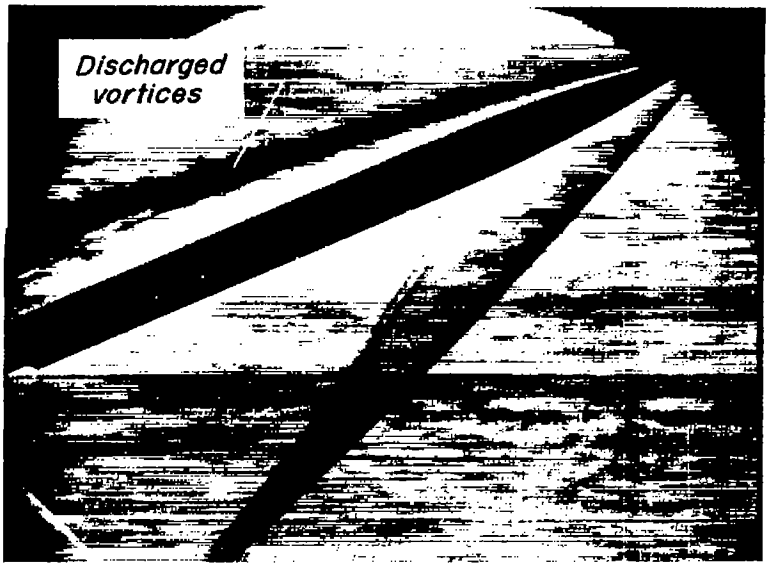

(a) Ogival-nosed body, $\alpha = 25°$

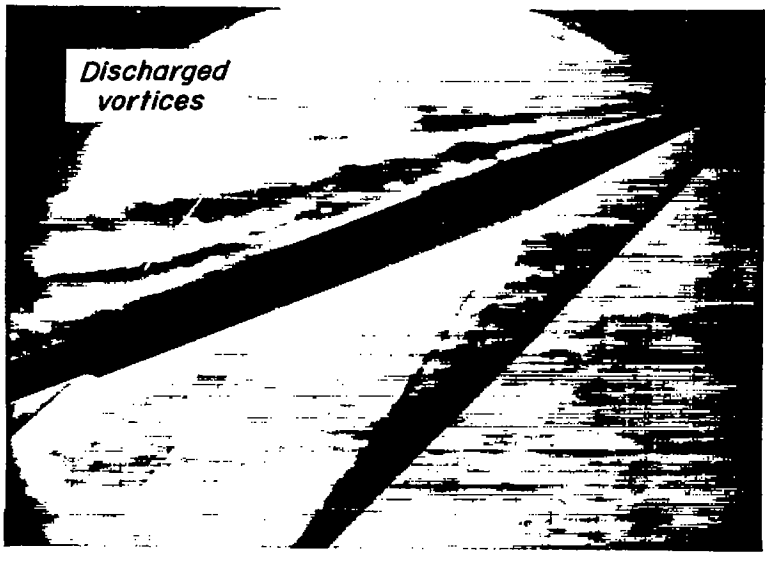

(b) Conical-nosed body, $\alpha = 24°$.

NACA
A-17641

Figure 8.- Schlieren photographs showing the cross-flow vortices in the lee of two bodies of revolution. $M_\infty = 1.45$, $Re = 0.5 \times 10^6$.

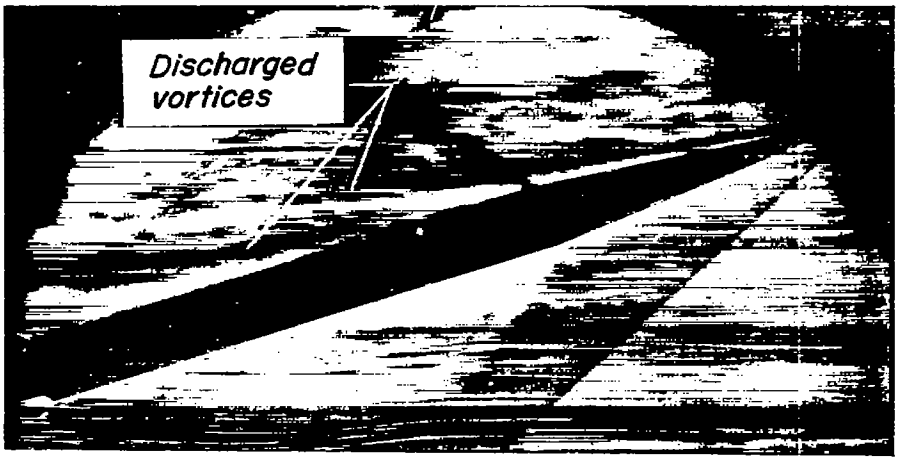

(a) Reference angle, $\theta = 0°$.

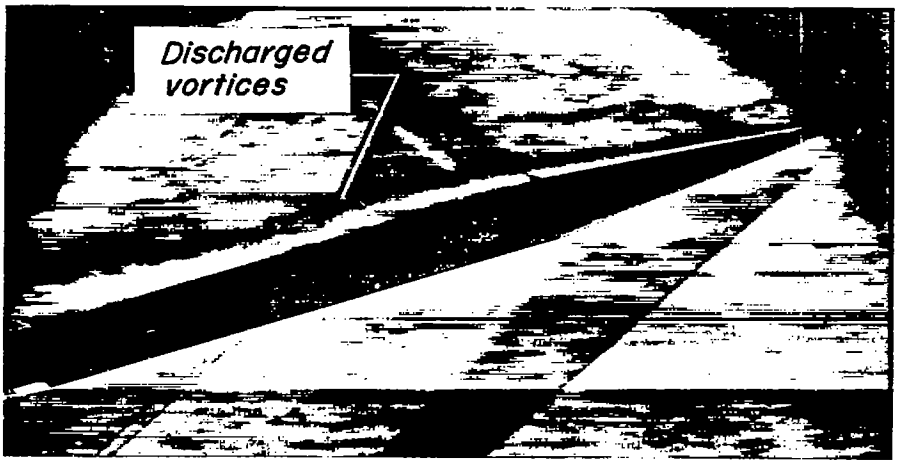

(b) Reference angle, $\theta = 10°$.

NACA
A-17642

Figure 9.– Schlieren photographs showing different vortex configurations for two angles of roll for the conical–nosed body at an angle of attack of 18°. $M_o = 1.45$, $Re = 0.5 \times 10^6$.

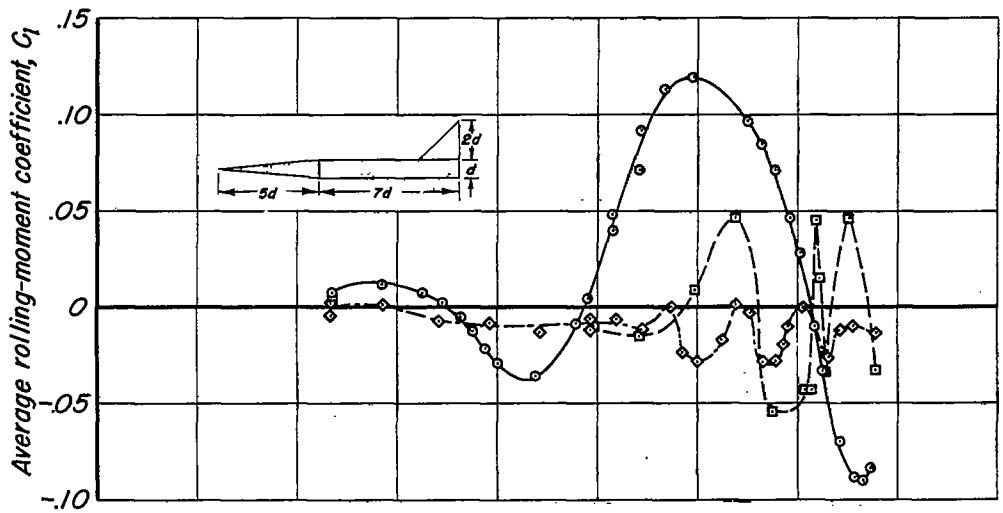

(a) Average rolling-moment coefficient.

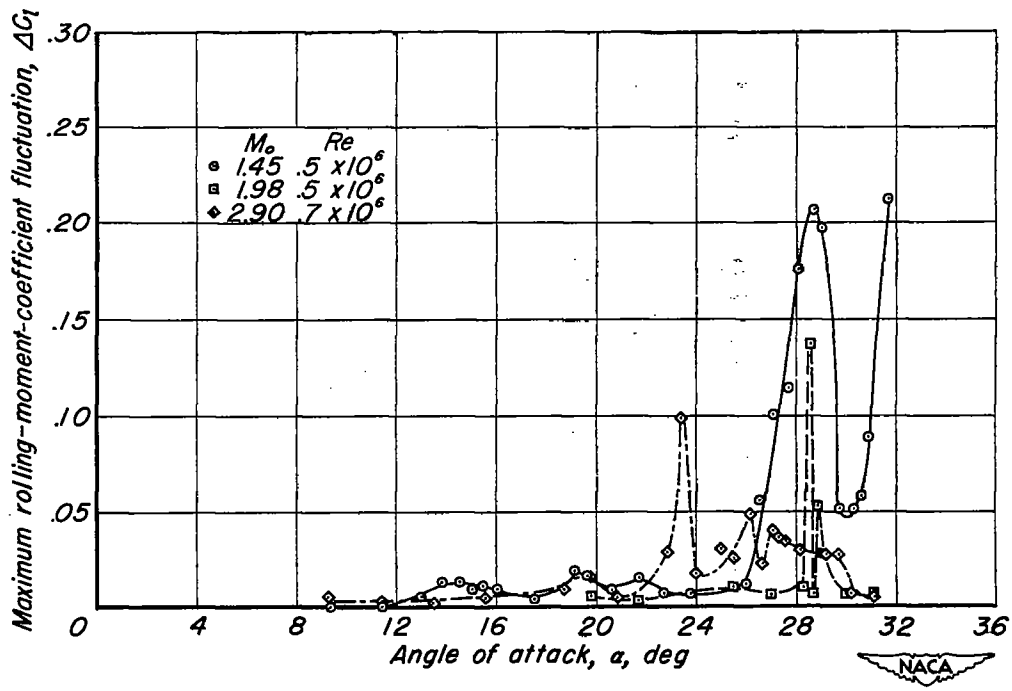

(b) Maximum rolling-moment-coefficient fluctuation

Figure 10.–Variation of the average and the maximum-fluctuating components of rolling-moment coefficients with angle of attack for a body-tail combination with a conical nose.

[redacted]

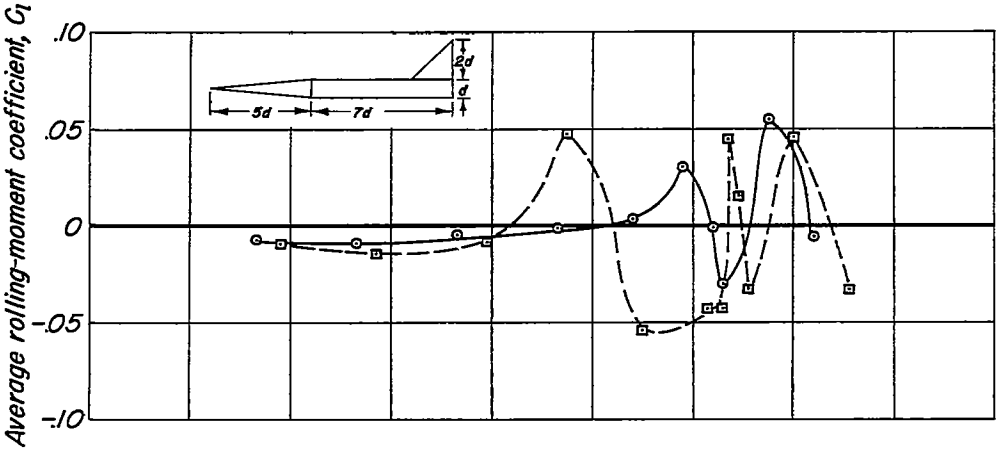

(a) Average rolling-moment coefficient

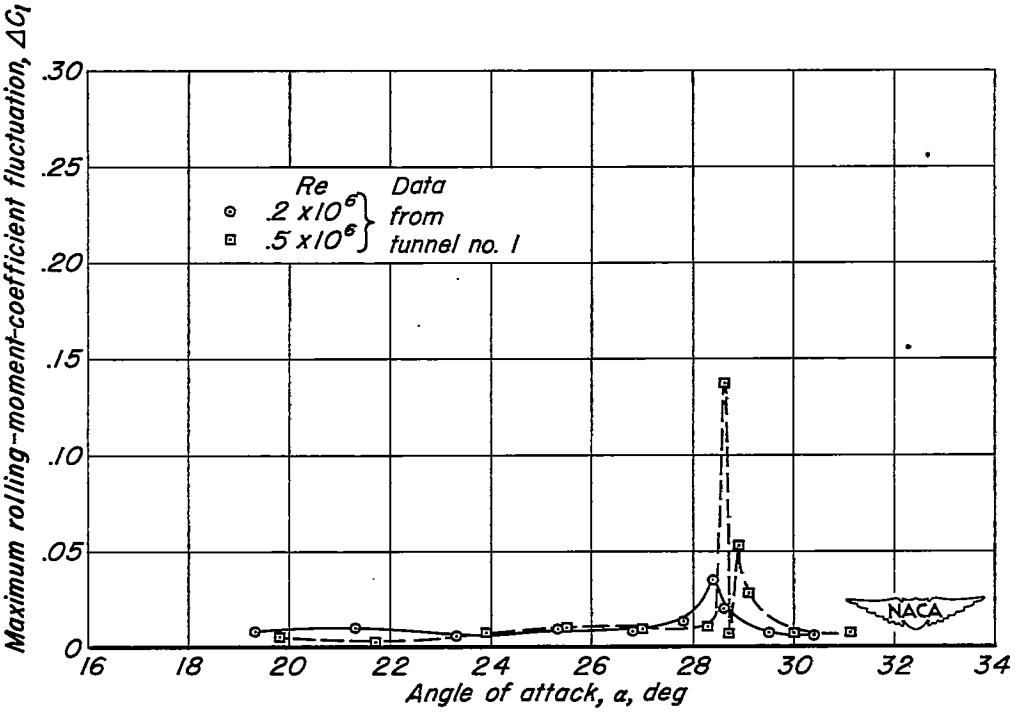

(b) Maximum rolling-moment-coefficient fluctuation.

Figure 11.- Effect of Reynolds number on the average and the maximum fluctuating components of rolling-moment coefficients for a body-tail combination with a conical nose at a Mach number of 1.98.

[redacted]

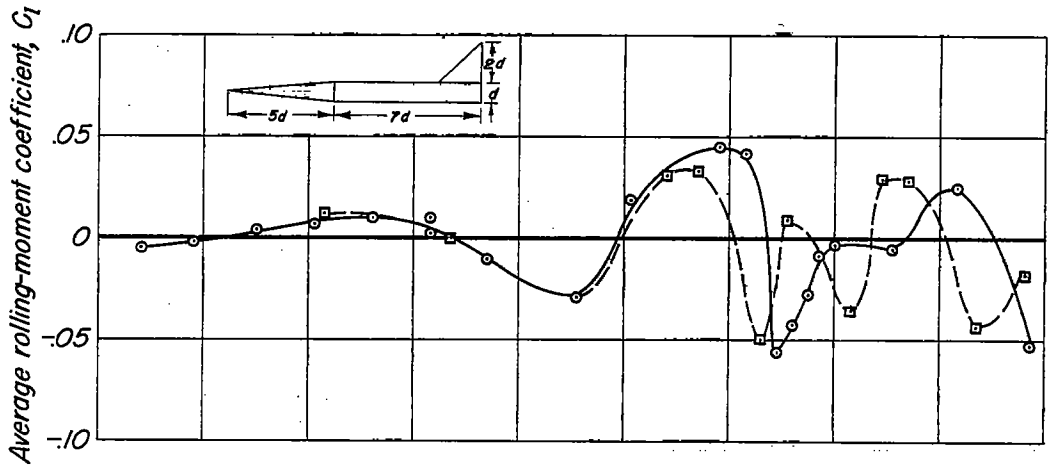

(c) Average rolling-moment coefficient.

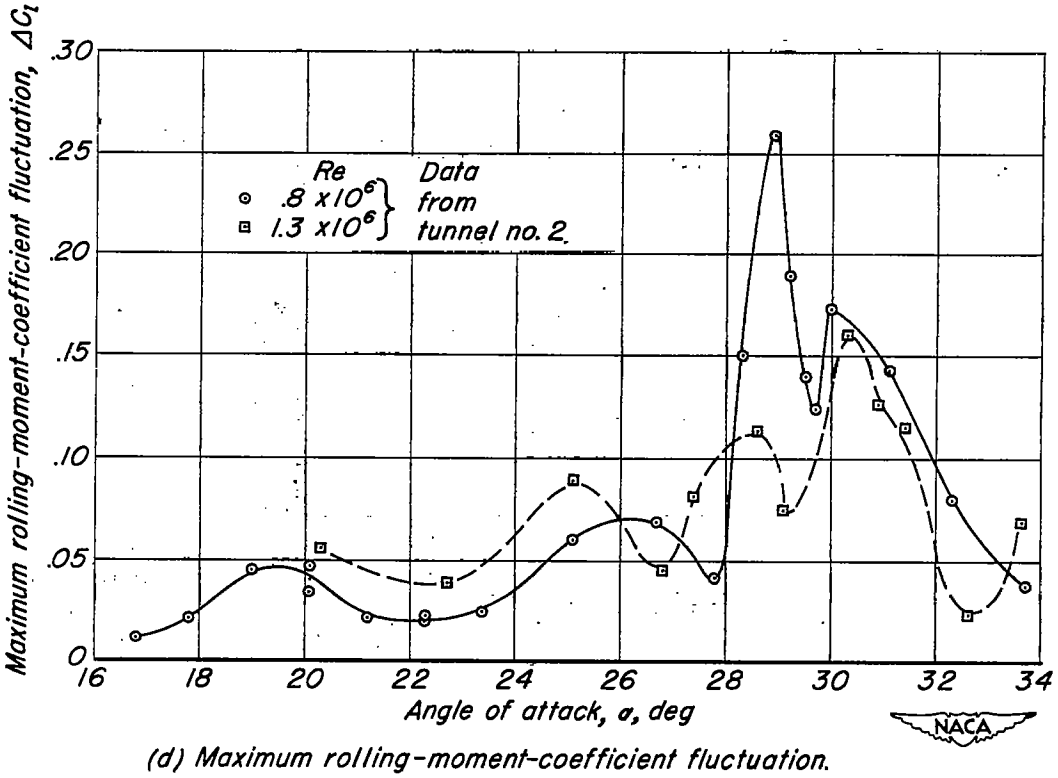

(d) Maximum rolling-moment-coefficient fluctuation.

Figure 11.- Concluded.

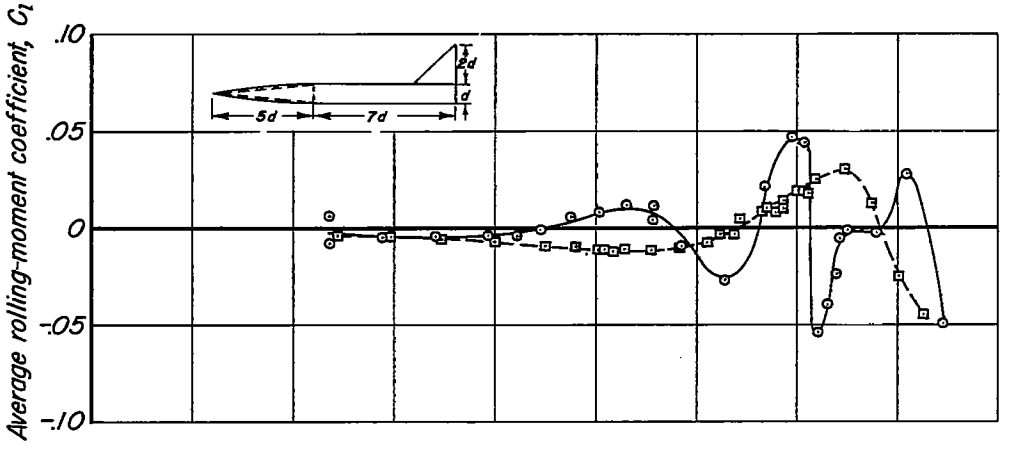

(a) Average rolling-moment coefficient

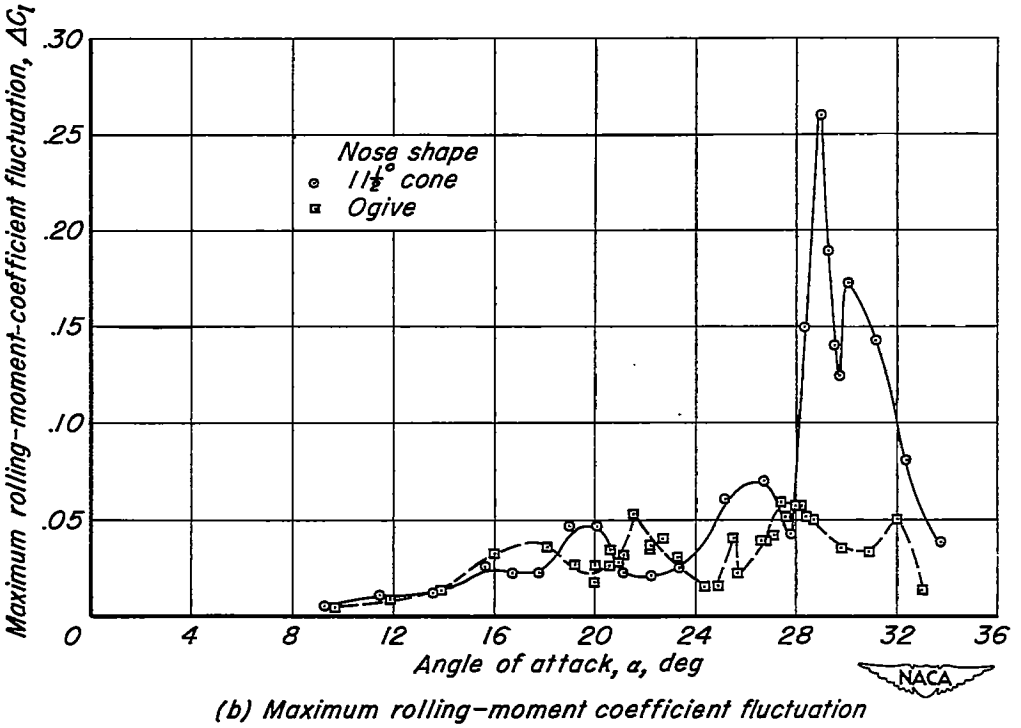

(b) Maximum rolling-moment coefficient fluctuation

Figure 12.–Effect of nose shape on the average and the maximum-fluctuating components of the rolling-moment coefficients for a body-tail combination. M_o=1.98, Re=0.8x10^6

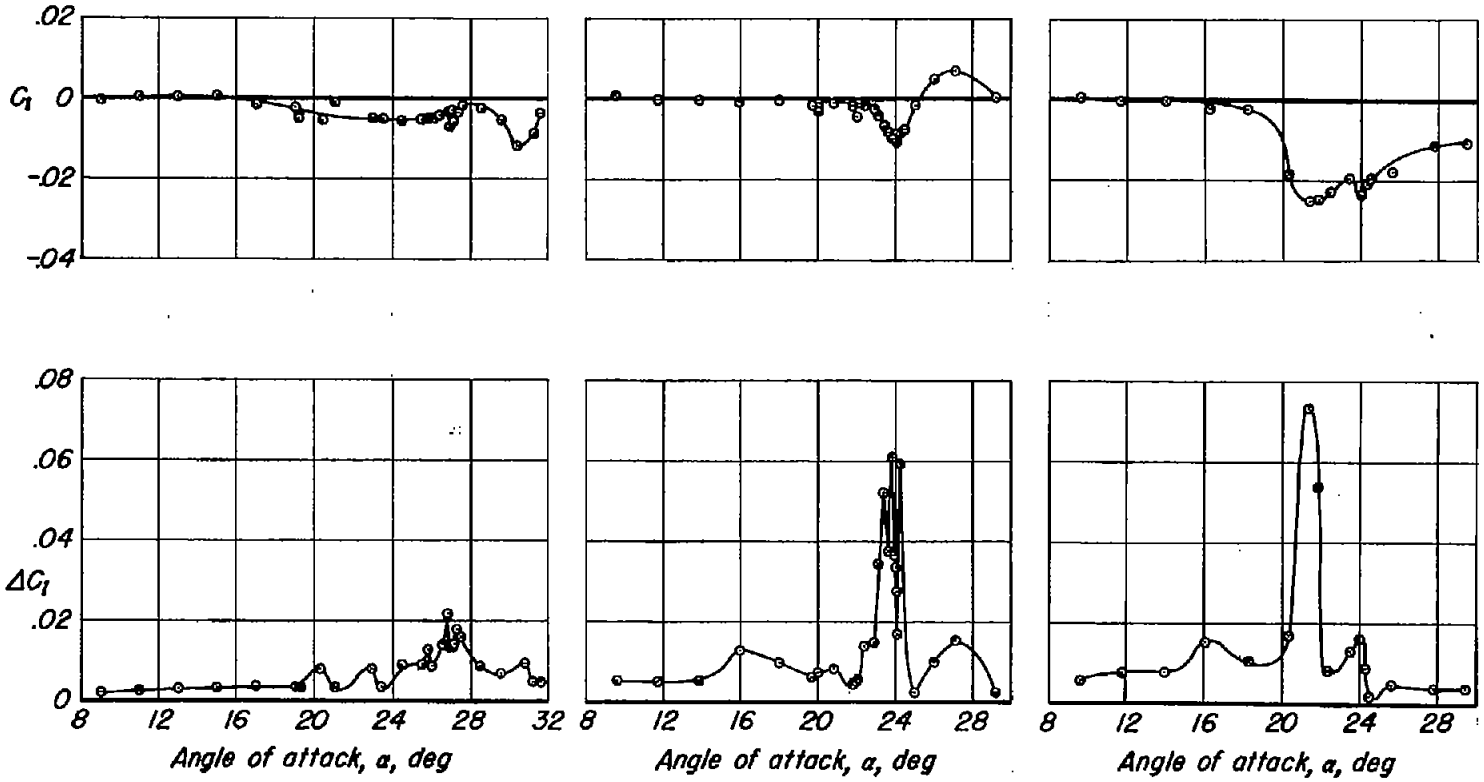

(a) Tail trailing edge 9.6 diameters from nose.

(b) Tail trailing edge 12.0 diameters from nose.

(c) Tail trailing edge 14.4 diameters from nose.

Figure 13.–Variation of the average and the maximum fluctuating components of the rolling-moment coefficients with angle of attack for three different tail positions on the body with an ogival nose. $M_\infty = 2.90$, $Re = 0.7 \times 10^6$.

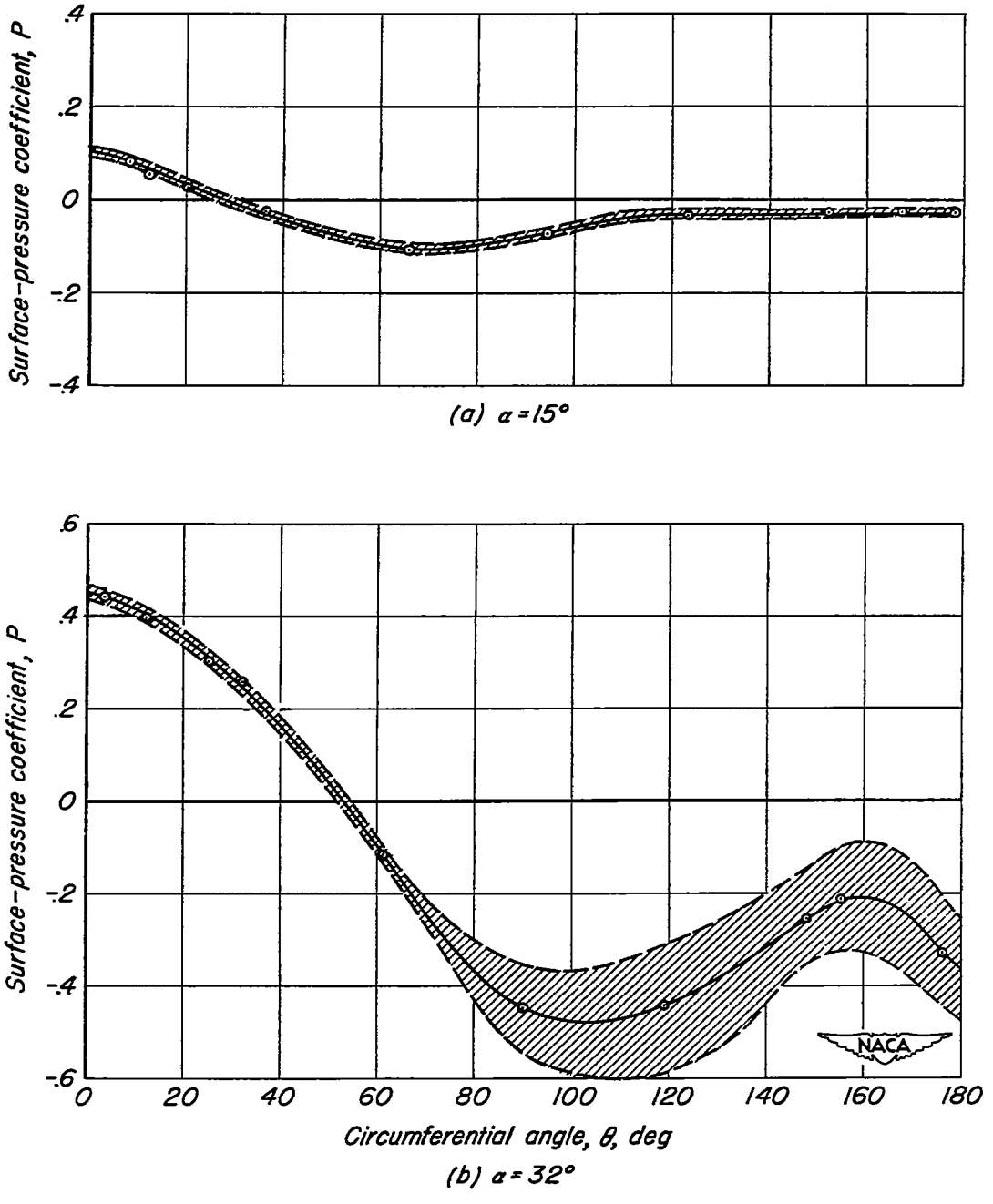

Figure 14.- Comparison of the average and fluctuating components of the surface-pressure coefficient at the 84-percent-length station on the conical-nosed body for two angles of attack. $M_\infty = 1.45$, $Re = 0.5 \times 10^6$.

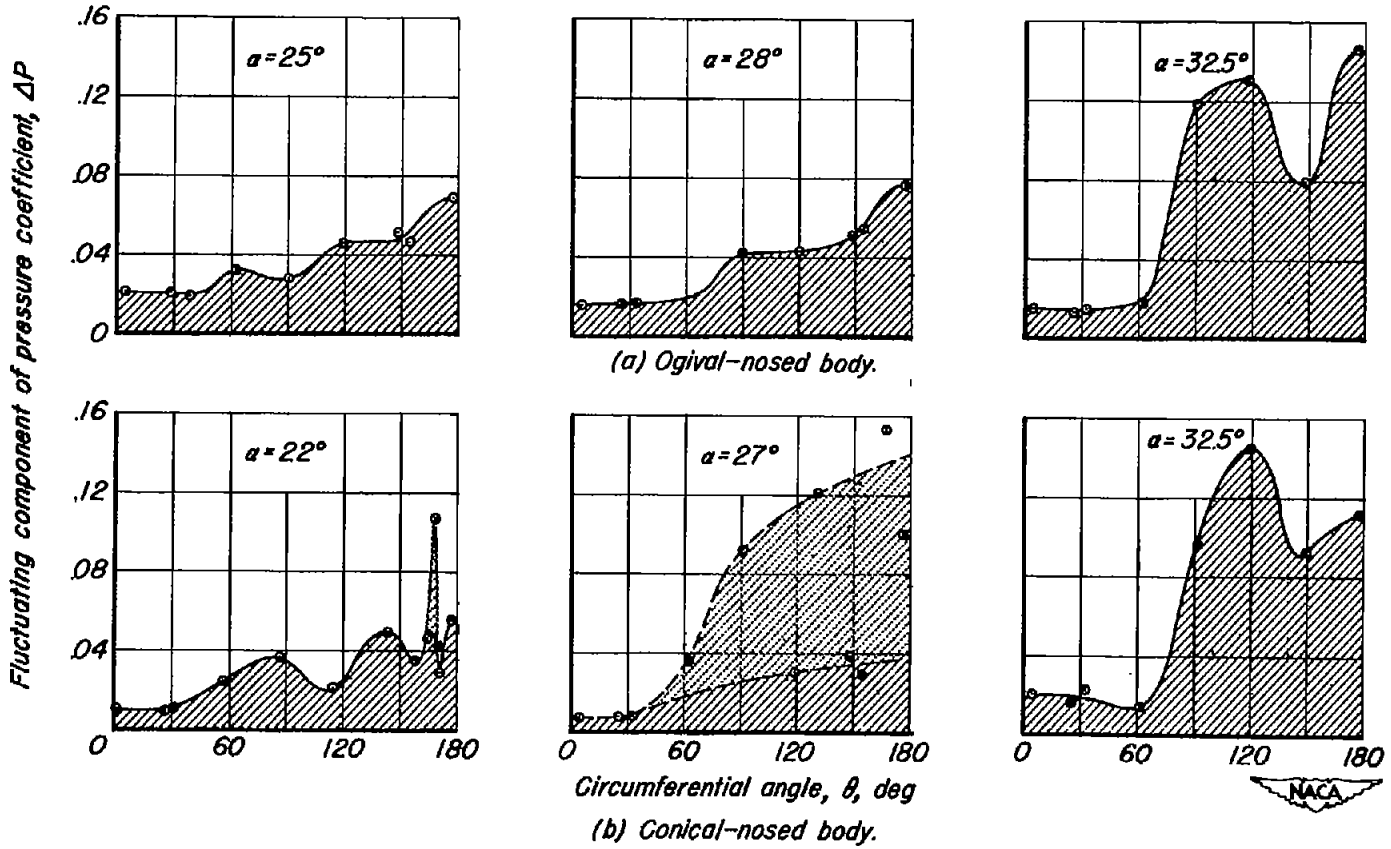

Figure 15.- Circumferential distributions of the fluctuating component of pressure coefficient for two bodies of revolution. $M_\infty = 1.45$, $Re = 0.5 \times 10^6$

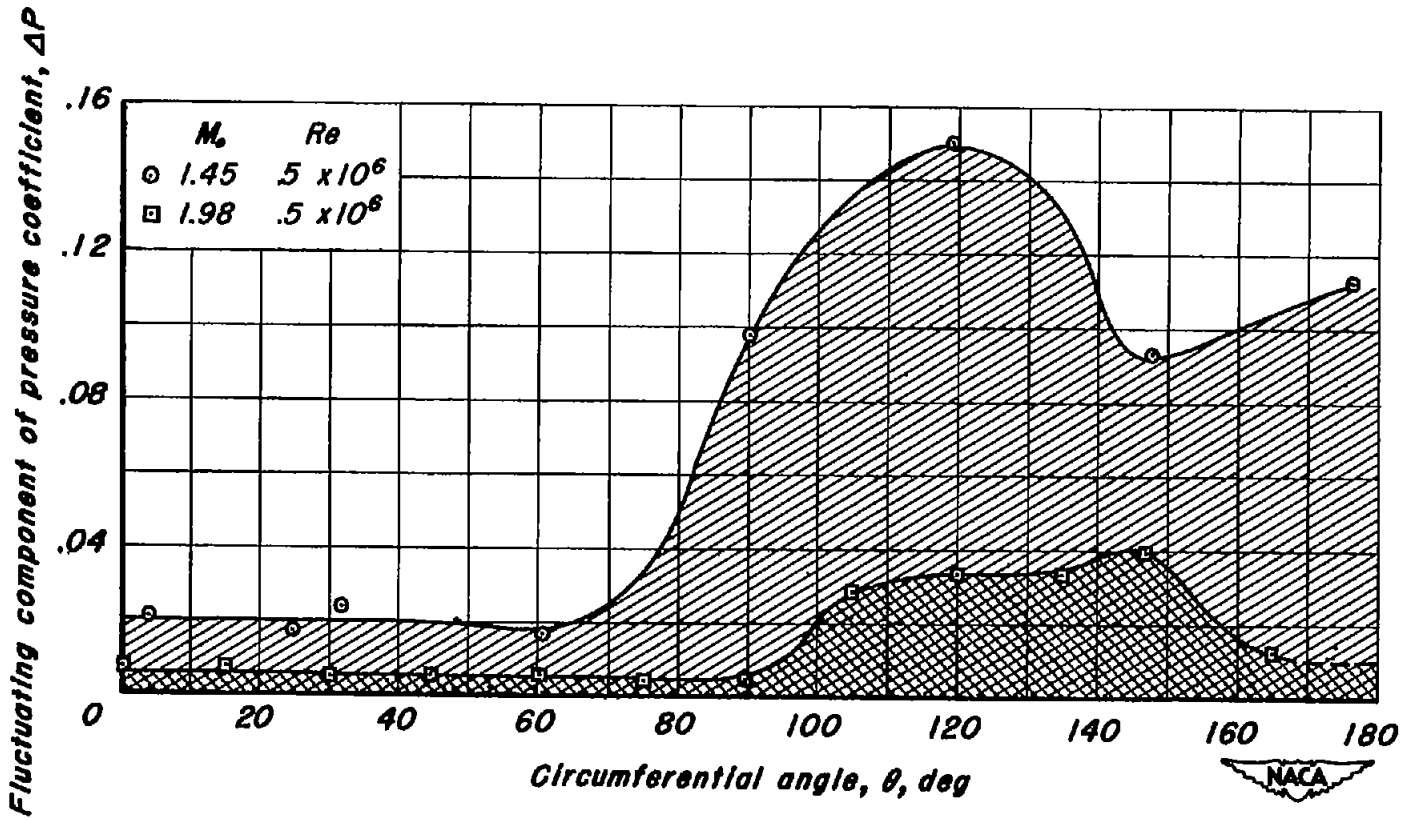

Figure 16.–Effect of Mach number on the circumferential distribution of the fluctuating component of pressure coefficient for the conical-nosed model at an angle of attack of 32.5°.